

Splice Variants of Na_v1.7 Sodium Channels Have Distinct β Subunit-Dependent Biophysical Properties

Clare Farmer¹, James J. Cox², E. V. Fletcher^{1*}, C. Geoffrey Woods³, John N. Wood², Stephanie Schorge^{1*}

1 UCL Institute of Neurology, Queen Square, London, United Kingdom, **2** UCL Wolfson Institute of Biomedical Research, London, United Kingdom, **3** Department of Medical Genetics, Cambridge Institute for Medical Research, Addenbrooke's Hospital, Cambridge, United Kingdom

Abstract

Genes encoding the α subunits of neuronal sodium channels have evolutionarily conserved sites of alternative splicing but no functional differences have been attributed to the splice variants. Here, using Na_v1.7 as an exemplar, we show that the sodium channel isoforms are functionally distinct when co-expressed with β subunits. The gene, *SCN9A*, encodes the α subunit of the Na_v1.7 channel, and contains both sites of alternative splicing that are highly conserved. In conditions where the intrinsic properties of the Na_v1.7 splice variants were similar when expressed alone, co-expression of β 1 subunits had different effects on channel availability that were determined by splicing at either site in the α subunit. While the identity of exon 5 determined the degree to which β 1 subunits altered voltage-dependence of activation ($P=0.027$), the length of exon 11 regulated how far β 1 subunits depolarised voltage-dependence of inactivation ($P=0.00012$). The results could have a significant impact on channel availability, for example with the long version of exon 11, the co-expression of β 1 subunits could lead to nearly twice as large an increase in channel availability compared to channels containing the short version. Our data suggest that splicing can change the way that Na_v channels interact with β subunits. Because splicing is conserved, its unexpected role in regulating the functional impact of β subunits may apply to multiple voltage-gated sodium channels, and the full repertoire of β subunit function may depend on splicing in α subunits.

Citation: Farmer C, Cox JJ, Fletcher EV, Woods CG, Wood JN, et al. (2012) Splice Variants of Na_v1.7 Sodium Channels Have Distinct β Subunit-Dependent Biophysical Properties. PLoS ONE 7(7): e41750. doi:10.1371/journal.pone.0041750

Editor: Jon T. Brown, University of Bristol, United Kingdom

Received: April 17, 2012; **Accepted:** June 25, 2012; **Published:** July 24, 2012

Copyright: © 2012 Farmer et al. This is an open-access article distributed under the terms of the Creative Commons Attribution License, which permits unrestricted use, distribution, and reproduction in any medium, provided the original author and source are credited.

Funding: SS holds a University Research Fellowship from the Royal Society. This work was funded by the MRC (CF, JJC, JNW, SS), BBSRC (JJC, JNW), and Wellcome Trust (JJC, CGW, JNW, SS), and World University Program grant R31-2008-000-10103-0 (JNW). The funders had no role in study design, data collection and analysis, decision to publish, or preparation of the manuscript.

Competing Interests: The authors have read the journal's policy and have the following conflicts: Funding was received from Pfizer (JJC, CGW). This does not alter the authors' adherence to all the PLoS ONE policies on sharing data and materials.

* E-mail: s.schorge@ucl.ac.uk

‡ Current address: Department of Pathology, Center for Motor Neuron Biology and Disease, Columbia University, New York, New York, United States of America

Introduction

As with other neuronal TTX-sensitive sodium channels, *SCN9A* is subject to alternative splicing at least at two sites. The gene contains two alternate mutually exclusive exons (5A and 5N) encoding the extracellular linker and voltage-sensor in the first domain, a feature shared with most neuronal sodium channels (Figure 1A; [1]). Along with other sodium channels [2,3,4], splicing of exon 5 is developmentally regulated in *SCN9A* [5]. The second conserved splicing site is an alternate recognition sequence at the end of exon 11 that allows a short (11 S) or long (11 L) intracellular linker to be produced between domains I and II of the channel (Figure 1A; [6,7]). Again there is a developmental change in expression with adult dorsal root ganglion (DRG) neurons showing increased levels of 11L compared to neonatal neurons [5]. Splicing at exon 11 has recently been shown to alter the sensitivity of the channel to phosphorylation [6], suggesting that splicing may modulate the sensitivity of the channel to intracellular regulation, but the interaction between the splice variants and accessory subunits has not been investigated.

Sodium channels are thought to be composed of multiple subunits, with β subunits modulating the expression, localisation and gating of the channels. β subunits are already recognized as potential therapeutic targets [8], but it is unclear what determines

their assembly with different α subunits. The dynamic regulation of β subunits during development [9] and diseases such as epilepsy [10], suggests that these subunits may not be constitutively present in sodium channel complexes. Moreover the different regulation of splicing and β subunit expression in development and disease suggests that different splice variants may associate with different β subunits.

The voltage-gated sodium channel Na_v1.7 plays an important role in nociception in peripheral sensory neurons [11,12]. Changes in the activity of the channel can have striking and specific effects on sensitivity to pain. Homozygous loss of function mutations in *SCN9A*, the gene which encodes the α subunit of Na_v1.7, is associated with inability to feel pain [13], while mutations that increase channel function lead to disorders characterised by extreme pain [14,15,16]. Because of its importance in pain, there is potential clinical relevance for factors that modify the activity of Na_v1.7 channels. Two possible factors which could modulate the channel during development and disease are alternative splicing and assembly with accessory subunits.

We asked whether different splice variants could interact differently with a β subunit to modify the gating of Na_v1.7 channels. As proof of principle we have focused on β 1 subunits, which are not covalently linked to α subunits, and which are downregulated in some neurological disorders [10,17]. Our data

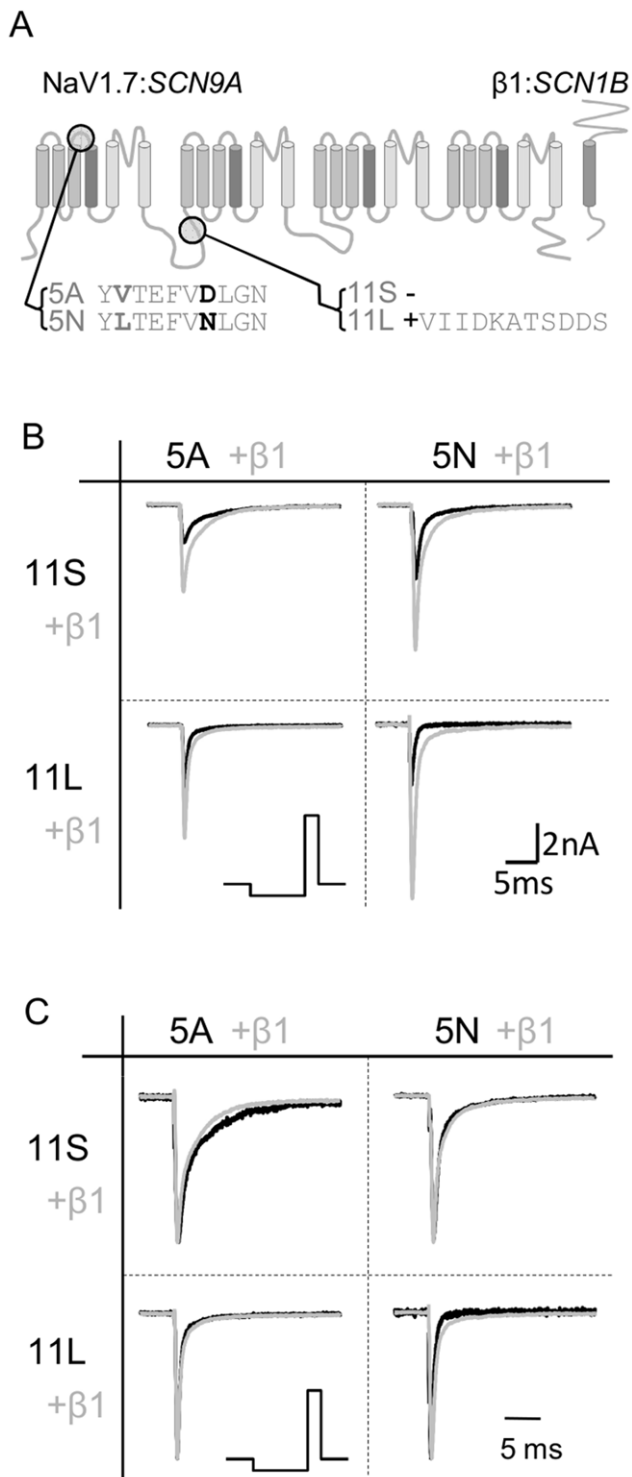


Figure 1. Overview of sites of splicing and channel behaviour. (A) A schematic of the α subunit of the $\text{Na}_v1.7$ channel with the location of the two changes introduced by splicing indicated. (B) Example traces from each of the splice variants in the absence (dark lines) and presence (grey lines) of $\beta 1$ subunits. Currents were elicited by a voltage step to -10 mV from a 100 ms prepulse to -120 mV to remove inactivation (protocol shown below). (C) Traces from (B) scaled to show a lack of effect of $\beta 1$ on the kinetics of α subunit inactivation and persistent current.

doi:10.1371/journal.pone.0041750.g001

suggest that $\beta 1$ subunits interacting with different α subunit splice variants could provide meta-regulation of channel gating.

Methods

Constructs

The four *SCN9A* constructs (5A11S, 5N11S, 5A11L, 5N11L) were cloned using standard molecular techniques and comprised the *SCN9A* clone (NM_002977) in a modified pcDNA3 vector followed by a polio IRES-DsRed2 fragment which permitted identification of transfected cells. Human sodium channel $\beta 1$ was amplified from human brain total RNA and cloned into the TOPO-directional vector (Invitrogen). All primer sequences are available upon request.

Cell Transfection

HEK293 (ATCC) cells were transfected with *SCN9A* constructs using lipofectamine 2000 (Invitrogen) and plated onto poly-d-lysine coated coverslips. All recordings were done 24–72 hours after transfection. Cells expressing $\text{Na}_v1.7$ were identified using red fluorescence, and cells co-expressing $\beta 1$ and GFP showed both red and green fluorescence. The amount of *SCN9A* DNA transfected remained constant throughout all experiments and when $\beta 1$ and GFP (pTracer, Invitrogen) were cotransfected it was in a ratio of 3:1:1 (*SCN9A*: $\beta 1$:GFP).

Electrophysiology

Whole-cell voltage clamp recordings were performed using an Axopatch 200 B amplifier at room temperature using standard techniques. Extracellular solution comprised (mM) NaCl 145, KCl 4, CaCl_2 1.8, MgCl_2 1, HEPES 10, (pH 7.35 with NaOH); intracellular (mM) CsCl 150, EGTA 10, HEPES 10, (pH 7.35 with CsOH). Data was sampled at 50 kHz, filtered at 5 kHz and leak currents were subtracted using a P/4 protocol. Average series resistance was $5.1 \pm 0.3 \text{ M}\Omega$ and was compensated by 75–90%. Tau of inactivation was measured by fitting a standard exponential function to the decaying current and persistent current was determined by measuring the current 20 ms after the start of the voltage step and expressing it as a percentage of the transient current in the same step. To assess voltage dependence of activation current-voltage families were obtained and peak sodium currents measured at each voltage. Channel conductance was calculated using the formula $G_{\text{Na}} = I / (V - V_{\text{rev}})$ where G_{Na} is sodium conductance, I is peak current, V is the voltage step and V_{rev} is the measured reversal potential which was determined for each cell by fitting a straight line through the linear portion of the current-voltage relationship. Sodium conductances were normalized and fitted with a standard Boltzmann function: $G_{\text{Na}} / G_{\text{Na,max}} = 1 / (1 + \exp((V_{50} - V) / k))$ where $G_{\text{Na}} / G_{\text{Na,max}}$ is the normalized conductance, V_{50} is the voltage which produces half maximal conductance and k is the slope factor. To reduce the risk of voltage clamp error in the estimates, cells with activation slopes less than 4 were discarded from the analysis. The protocol used to assess the voltage dependence of inactivation produced biphasic inactivation curves in a number of cells (37/59). The curves consisted of a large and stable negative component and a smaller, more variable positive component. The latter reflects a proportion of $\text{Na}_v1.7$ -mediated current which is not fully inactivating, probably due to variations in the development of closed-state inactivation which can be slow in these channels [18]. In these cells a double Boltzmann curve was fitted using the following function: $I_{\text{Na}} = A / (1 + \exp((C - V) / K)) + (1 - A) / (1 + \exp((D - V) / L))$ where A is a scaling factor, C and D are V_{50} values and K and L are slope factors of the two components of the fit. To improve the

quality of the fit D and L (V_{50} and slope of minor component) were fixed. This equation was manually entered into the GraphPad Prism non-linear curve fitting software. The V_{50} values for the more negative component were combined with the V_{50} values obtained for single Boltzmann fits from the remaining cells in order to compare the voltage dependence of inactivation between splice variants. Data was acquired and analysed using Labview software with programs written in house (DM Kullmann, UCL). Additional data analysis and statistical testing was performed using Clampfit, Microsoft Excel, Microcal Origin Pro, and GraphPad Prism software. All data is presented as mean \pm SEM.

Results

In individual neurons, multiple sodium channel α and β subunits may be co-expressed, and each α subunit may be present as a mixture of splice variants. In order to determine whether the β subunits had specific interactions with different splice variants of an α subunit, we used a line of HEK293 cells, which we have previously shown to have negligible expression of endogenous α and β channel subunits [19]. At physiological temperatures, we have found that the modulation imposed by β subunits is obscured, and because we were interested in whether it is possible for alternative splicing in the α subunit to alter the effects of β subunit co-expression, we carried out recordings at room temperature where interactions are more apparent. Our goal was to test the hypothesis that alternative splicing in α subunits could change the gating properties affected by β subunit expression.

When expressed alone in HEK293 cells, all human $Na_v1.7$ splice variants produced comparable sodium currents, with no significant difference between the variants in peak current density, rate of inactivation, or persistent currents (for each parameter, $P > 0.1$; 1-way ANOVA; Figure 1; Table 1). When held at -80 mV the inactivation curves of the $Na_v1.7$ variants were characterised by a significant second component, representing $18 \pm 2\%$ of the total current, which inactivated at more depolarised potentials (approximately -30 mV). We confirmed that when recording using intracellular solutions containing CsF, this component was suppressed (data not shown), suggesting it may be in part due to intracellular signalling. In order to improve the fit to the main component of inactivation when using solutions that did not contain fluoride, the V_{50} and slope of this second component were fixed, and only the fraction was allowed to vary. In all variants and subunit combinations, the percentage of current mediated by this component was similar ($P = 0.39$; 1-way ANOVA).

Table 1. Macroscopic gating properties of *SCN9A* splice variants with and without $\beta 1$ subunits.

cDNAs	n	INaT (pA/pF)	INaP (%INaT)	Tau _{inac} (ms)
5A11S	6	-105 ± 50	3.7 ± 2.0	1.15 ± 0.22
+ $\beta 1$	6	-260 ± 58 ‡	3.3 ± 1.0	1.78 ± 0.50
5N11S	10	-250 ± 64	2.7 ± 0.6	0.97 ± 0.15
+ $\beta 1$	7	-362 ± 83 ‡	2.9 ± 0.6	1.13 ± 0.33
5A11L	9	-207 ± 42	3.0 ± 1.1	0.99 ± 0.25
+ $\beta 1$	7	-321 ± 67 ‡	1.9 ± 0.3	0.78 ± 0.14
5N11L	6	-151 ± 26	2.7 ± 1.0	0.89 ± 0.32
+ $\beta 1$	8	-453 ± 80 ‡	1.9 ± 0.5	0.67 ± 0.09

‡ values with $\beta 1$ are significantly larger than without after 2-way ANOVA.
doi:10.1371/journal.pone.0041750.t001

Co-expression with the $\beta 1$ subunit consistently increased the mean peak currents, and this was highly significant overall ($P = 0.00057$, 2-Way ANOVA), with no significant differences between the current densities driven by splicing ($P = 0.20$ all 4 variants, 2-Way ANOVA). In contrast, the co-expression of $\beta 1$ subunits had no overall effect on the rate of inactivation or persistent current for the different splice variants (Table 1, $P > 0.1$, One-way ANOVA).

The $\beta 1$ subunits induced a slight hyperpolarizing shift in the voltage dependence of activation for all four splice variants, with the two variants containing the 5 N exon tending to larger shifts, independent of which exon 11 splice form was present (Figure 2, Table 2). Voltage dependence of inactivation was also altered, with the $\beta 1$ subunits producing a depolarising shift in the inactivation curves. However, in this case the identity of exon 11 appeared the driving factor, with variants containing exon 11 L having a larger shift than those containing exon 11 S, and the identity of exon 5 not appearing to alter inactivation (Table 2). Thus co-expression of $\beta 1$ subunits may combine with splicing in different domains of the channels to selectively alter different parameters of channel gating.

We hypothesized that the effects of exon 5 on activation could be uncoupled from the effects of exon 11 on inactivation, and to test this we pooled data from exon 11 L and 11 S cells to ascertain the effects of exon 5 on activation, and pooled the data from exon 5A and 5N cells to isolate the effects of exon 11 on inactivation.

Pooling cells according to exon 5 revealed that $\beta 1$ co-expression produced a larger hyperpolarising shift in activation for those containing 5N compared to 5A, regardless of exon 11 background (Figure 2, right column). While co-expression of $\beta 1$ shifted the activation of channels containing exon 5N an average of 5.1 mV (from -10.2 ± 0.5 to -15.3 ± 1.4 mV) it only changed the activation of channels containing 5A on average by less than 1 mV (0.8 mV; from -12.1 ± 0.9 mV to -12.9 ± 1.0). In total, the shift imposed by $\beta 1$ on 5N-containing channels was significantly larger than that on 5A-containing channels ($p(\Delta 5N = \Delta 5A) = 0.027$; 2-way ANOVA).

The effects on inactivation were more pronounced, and more closely driven by the length of exon 11. The $\beta 1$ -mediated depolarising shift in inactivation, when pooled according to exon 11 variant, showed that cells with the long variant had a much larger shift than cells containing the short variant, regardless of the identity of exon 5 (Figure 2, bottom row). While the presence of $\beta 1$ depolarised the inactivation of channels with the short exon by an average of 4.5 mV (from -82.1 ± 0.9 to -77.5 ± 1.7 mV) the shift in inactivation of channels containing exon 11 L was greater than 10 mV, or an average of 14.6 mV (from -87.2 ± 1.1 to -72.7 ± 1.2 mV). The change was significantly much larger in 11 L channels than those containing 11 S ($p(\Delta 11 L = \Delta 11 S) = 0.00012$; 2-way ANOVA).

The shift in inactivation introduced by $\beta 1$ subunits in the presence of exon 11 L introduced potentially important changes in channel availability near typical resting membrane potentials. For example, variant 5N11L changes from more than 60% inactivated at -80 mV in the absence of $\beta 1$ subunits to less than 20% inactive when $\beta 1$ is co-expressed, indicating that the presence of $\beta 1$ alters the availability of nearly half the channels at physiological resting potentials. However a direct prediction of channel availability during voltage steps may be confounded by a changing voltage dependence of activation, such as that caused by splicing of exon 5, or by altered trafficking in the presence of $\beta 1$ subunits. We therefore measured the current densities generated by the different splice variants over a range of potentials in the presence and absence of $\beta 1$ subunits when cells were held near physiological resting potential (Figure 3).

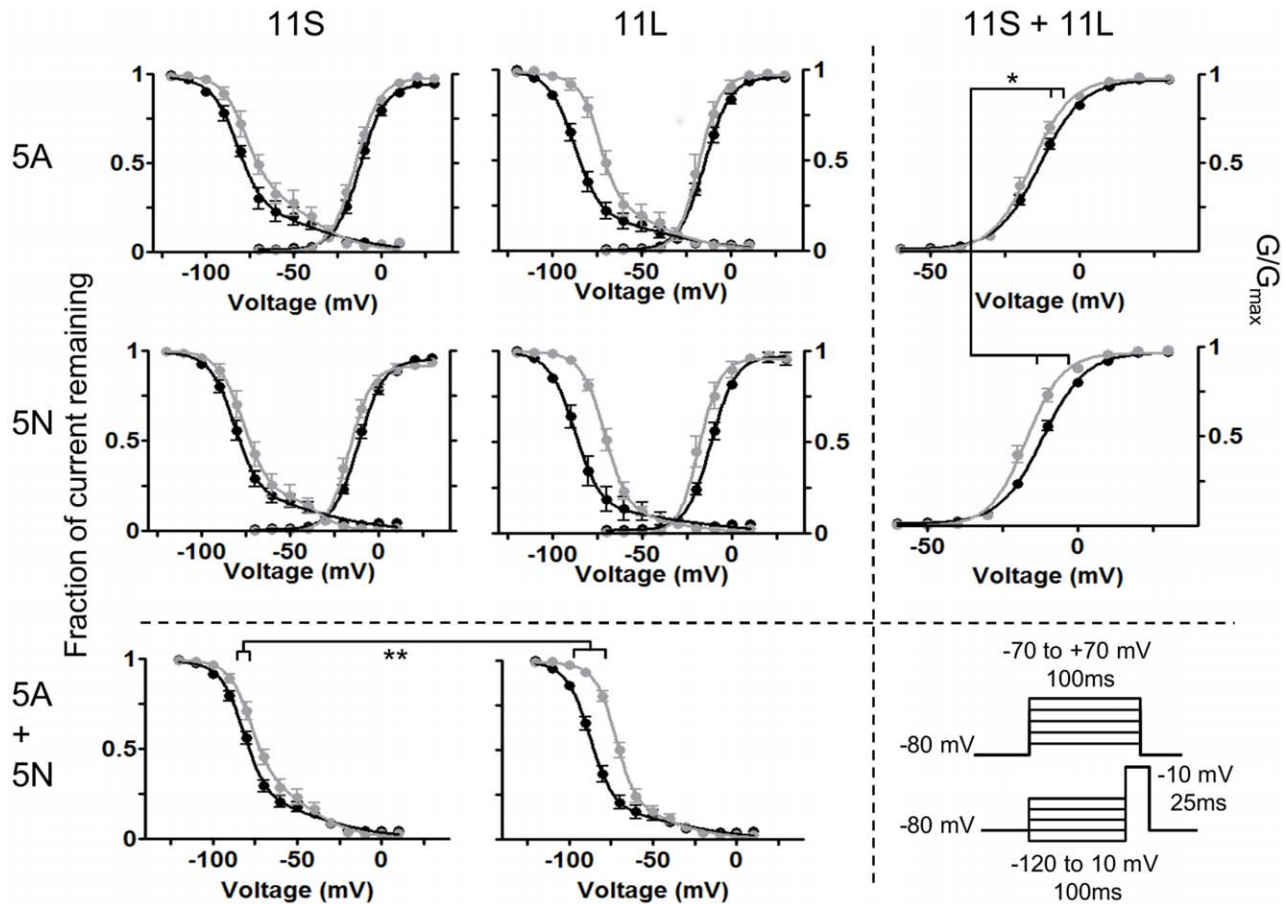


Figure 2. Exon 5 is preferentially coupled with activation and exon 11 modifies inactivation. Black lines are *SCN9A* alone, and grey lines are with $\beta 1$ subunits. The columns are arranged according to the length of exon 11, and rows by identity of exon 5. The bottom row shows pooled data from each exon 5 variant (irrespective to exon 11 length). The right column shows pooled data for each form of exon 11 (independent of identity of exon 5). Numbers of cells are as in the table. Voltage protocols are shown for activation (top) and inactivation (bottom). doi:10.1371/journal.pone.0041750.g002

When current densities for the different variants were systematically compared over a range of potentials, the different splice variants revealed patterns of increased current density that were consistent with exon 5 targeting activation and exon 11

altering availability by shifting steady state inactivation. Variants with the 'long' version of exon 11, had larger increases than 11 S variants over a range of strongly depolarized potentials (0 to +40 mV, Figure 3B bottom), suggesting that the change in inactivation had a significant effect on channel availability when stepped from -80 mV to a range of potentials. The splicing at exon 5, in contrast, altered the amplitude of currents at more hyperpolarized potentials (-40 to -20 mV, Figure 3B, top), with no effect on the strongly depolarized currents (0 mV and above), which is consistent with the larger effect on activation and little effect on channel availability at the initial -80 mV holding potential. The combination of splicing and $\beta 1$ subunits meant that the largest shift, given by exon 5 N combined with the long form of exon 11 gave over a 6 fold increase in current density at -20 mV, while the opposite combination of exon 5A with short exon 11 gave just over 2-fold increase at the same potential.

Taken together, our results suggest that $\beta 1$ subunits interact differently with $Na_v 1.7$ channels encoded by different splice variants of *SCN9A* and can differentially regulate channel availability at resting potentials and during activation with large effects on channel availability and activation.

Table 2. Voltage dependent parameters of *SCN9A* splice variants with and without $\beta 1$ subunits.

cDNAs	n	Activation		Inactivation	
		V_{50}	Slope	V_{50}	Slope
5A11S	15	-11.0 ± 1.0	7.5 ± 0.4	-83.0 ± 1.4	-7.1 ± 0.5
+ $\beta 1$	12	-13.1 ± 1.4	6.9 ± 0.4	-78.3 ± 2.8	-5.6 ± 0.5
5N11S	13	-10.0 ± 0.7	8.0 ± 0.5	-81.5 ± 1.3	-6.5 ± 0.3
+ $\beta 1$	10	$-15.8 \pm 1.8^*$	6.1 ± 0.6	-76.8 ± 2.2	-6.0 ± 0.4
5A11L	9	-14.4 ± 1.5	7.0 ± 0.4	-87.3 ± 1.4	-6.8 ± 0.1
+ $\beta 1$	7	-12.4 ± 1.2	6.1 ± 0.4	$-74.1 \pm 1.3^{**}$	-5.8 ± 0.7
5N11L	7	-10.5 ± 0.6	7.3 ± 0.5	-87.3 ± 1.8	-7.0 ± 0.5
+ $\beta 1$	7	-14.6 ± 2.4	6.2 ± 0.6	$-71.5 \pm 2.0^{**}$	-5.5 ± 0.1

* $p < 0.05$, ** $p < 0.001$ compared to same splice variant without $\beta 1$ after 1-way ANOVA with Tukey-Kramer Multiple Comparisons Test. doi:10.1371/journal.pone.0041750.t002

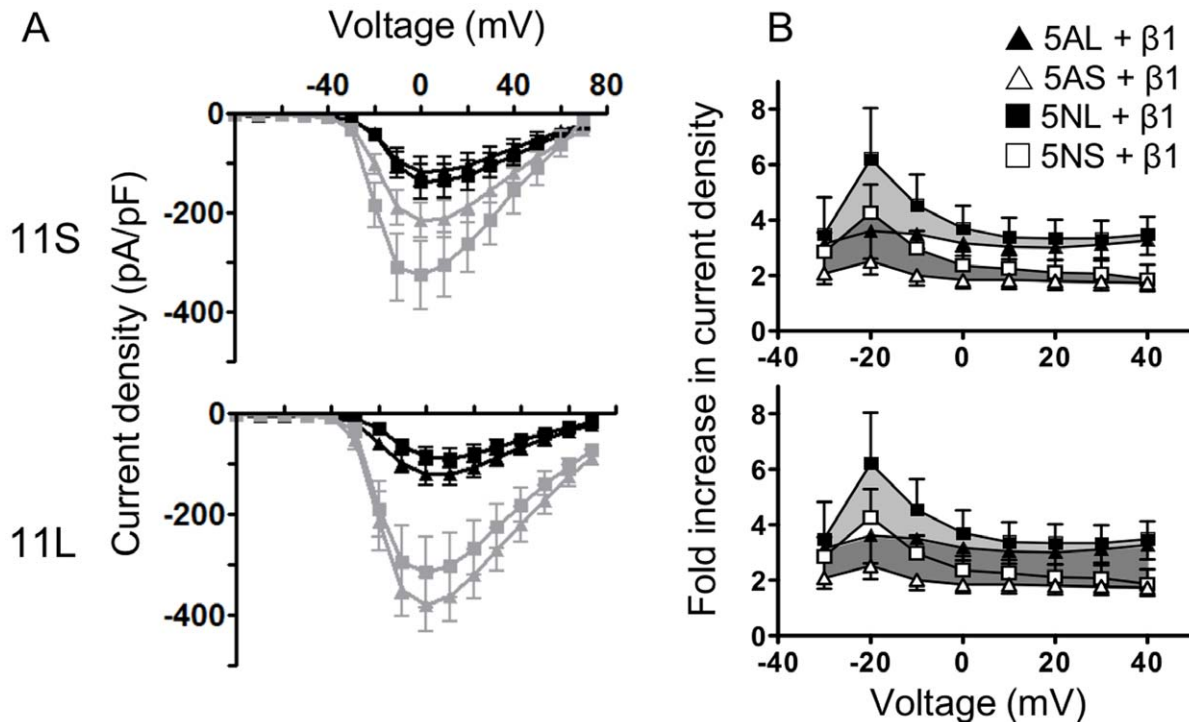


Figure 3. $\beta 1$ subunits have different effects on current densities depending on splicing in *SCN9A*. (A) Un-normalised current density plots showing increased current due to expression of $\beta 1$ subunits. Triangles = exon 5A, Squares = exon 5N. Grey = with $\beta 1$ subunits. To assess the impact of the β subunits we held cells at physiological potentials (-80 mV) and stepped to a range of potentials (-80 to $+70$ mV). (B) Consequences of $\beta 1$ subunit co-expression for steps to different potentials. The same data are shown in top and bottom panels, but in the top panel the greyed-out triangular area indicates the difference in current amplitude between variants that differ at exon 5, while in the bottom panel the shaded areas indicate the difference introduced by changing the length of exon 11. In contrast to the changes due to exon 5, which are much larger at -20 mV than at most other potentials, the changes imposed by exon 11 are of similar amplitude over the range of potentials tested. Exon 11 length (bottom panel) is associated with approximately a two fold increase of current density over all voltages. The identity of exon 5 induces a specific increase (~ 2 fold) in the neighbourhood of -20 mV (top panel), but virtually no difference at more depolarised potentials. Cell numbers are as in Table 2. doi:10.1371/journal.pone.0041750.g003

Discussion

Meta-regulation of Sodium Channels by β Subunits and Alternative Splicing

Our data reveal that splicing at two sites within a sodium channel α subunit can change how $\beta 1$ subunits modulate the function of the channels. In the first domain of the α subunit, alternative splicing of exon 5, which changes the S3–S4 linker, modulates the effect of $\beta 1$ subunits on the voltage-dependence of activation. In contrast, the length of exon 11, which changes the first intracellular loop of the channel, determines the degree to which $\beta 1$ subunits shift the voltage-dependence of steady-state inactivation of the channels. These data suggest that the functional effects of splice variants can be modified by accessory subunits, and because alternative splicing in neuronal sodium channels is highly conserved [1], it is possible that similar interactions between splicing and accessory subunits may occur with other Na_V channels. Our data also indicate that the repertoire of β subunit functions can be expanded by considering their potential ability to discriminate between α subunit splice variants.

Our observations are consistent with work from other groups suggesting that in the presence of $\beta 1$ subunits there is little difference between macroscopic currents from *SCN9A* splice variants recorded from HEK cells held at strongly hyperpolarized potentials [6]. However, recording at more physiological potentials and varying accessory subunit expression reveals

significant differences between the behaviour of splice variants. These data suggest a meta-regulation – a second level of regulation of channel function – can be produced by the distinct interaction of different splice variants with with accessory subunits, and provide a new insight into how alternative splicing may modify the function of sodium channels. Because alternative splicing of sodium channels has been shown to be highly conserved [1], the four α subunit splice variants and one accessory subunit, *SCN1B*, that we have investigated here represent a small proportion of the possible combinations of splice variants and β subunits.

However, it is important to note that these data are only a proof in principle that β subunits might selectively interact with splice variants of the α subunits. We have recently shown that the effects of several β subunits on gating of a voltage-gated sodium channel are obscured at higher temperatures (see table 2 in [19]), and as we were most interested in dissecting the differences between a representative β subunit and the splice variants of *SCN9A* we carried out recordings at room temperature to maximise the sensitivity of detection. Moreover, the full function of β subunits is likely to be dependent on cellular background with many key β subunit functions appearing to be restricted to neurons [20], thus in order to determine the true functional importance of the different interactions, recordings would have to be done in a neuronal setting where the full functional roles of β subunits can be probed. Our data indicate that these recordings will require some

means of assessing which splice variants of α subunits are present prior to limiting β subunit.

Implications for SCN9A

We chose *SCN9A* because this encodes one of the sodium channel α subunits which has the most carefully aligned genotype/phenotype relationship [11]. For this channel it is known that relatively small shifts in current activation are sufficient to lead to clinically important effects. While caution is required in translating between currents seen in HEK cells and those expected in neurons, it is possible that small changes imposed by the co-expression of β subunits could have clinically significant effects. Recent work in $\beta 1$ knockout mice showing significant effects on the voltage-dependence of inactivation of TTX-sensitive currents in DRG neurons suggests $\beta 1$ subunits are present in these cells and may modify $\text{Na}_v1.7$ inactivation, albeit in the opposite direction seen in HEK cells [21]. Mutations in *SCN9A* which hyperpolarise $\text{Na}_v1.7$ activation (see e.g. [22,23,24]), or cause a gain of function by impairing fast-inactivation of $\text{Na}_v1.7$ channels (see e.g. [15,25]), can both cause diseases of pain in humans. It has already been suggested that splicing in *SCN9A* may alter the severity mutations in the gene [25], and our data suggest that accessory subunits may also contribute to functional differences between variants. Healthy human DRG express a mixture of all four $\text{Na}_v1.7$ splice variants, however the expression pattern has been shown to change in an animal model of nerve injury [7]. Our data suggest a role for accessory subunits in determining the consequences of these changes in splicing. This role may also be subject to regulation, because $\beta 1$ subunits themselves are dynamically regulated during development [9,26] and disease, including spinal cord injury [27].

Splicing Combines with Accessory Subunits to Uncouple Modulation of Activation and Inactivation

It is surprising that the presence of the $\beta 1$ subunit can significantly influence two different functional parameters for the

two $\text{Na}_v1.7$ splice variants, and suggest that in this system different regions of the channel may interact with the $\beta 1$ subunits. The effects of $\beta 1$ on inactivation in constructs containing the long form of exon 11 imply that there may be some interaction between $\beta 1$ and the intracellular loop between domains I and II in $\text{Na}_v1.7$ that contributes to the regulation of inactivation. This loop is partially coded for by exon 11 and is extended in length in the 11 L splice variant by 11 amino acids [6]. The altered activation of channels associated with splicing of exon 5 in the presence of $\beta 1$ subunits suggests the S3–S4 linker of the first domain and the extracellular domain of the $\beta 1$ subunits may also interact. Splicing at exon 5 consistently alters a single evolutionarily conserved charged amino acid in this short extracellular linker in the α subunit of several sodium channels [1], and it is possible this amino acid contributes to the altered interaction with $\beta 1$. In the related $\text{Na}_v1.1$ subunit, we found increasing temperature reduced the effects of β subunits [19]; this may indicate that the interactions seen in HEK cells are less stable than those in neurons.

This study provides the first evidence that evolutionary conserved splice variants of a voltage-gated sodium channel, in this case $\text{Na}_v1.7$, can interact in a functionally distinct fashion with sodium channel accessory subunits. The consequences of this interaction in neurons remains to be determined; this study nonetheless demonstrates a regulatory mechanism for sodium channel function dependent on accessory subunit interactions that may be relevant to the whole nervous system.

Acknowledgments

SS holds a University Research Fellowship from the Royal Society.

Author Contributions

Conceived and designed the experiments: CEF JJC EVF CGW JNW SS. Performed the experiments: CEF JJC EVF SS. Analyzed the data: CEF JJC EVF CGW JNW SS. Contributed reagents/materials/analysis tools: CEF JJC EVF SS. Wrote the paper: CEF JJC EVF CGW JNW SS.

References

- Copley RR (2004) Evolutionary convergence of alternative splicing in ion channels. *Trends Genet* 20: 171–176.
- Gazina EV, Richards KL, Mokhtar MB, Thomas EA, Reid CA, et al. (2010) Differential expression of exon 5 splice variants of sodium channel alpha subunit mRNAs in the developing mouse brain. *Neuroscience* 166: 195–200.
- Gustafson TA, Clevinger EC, O'Neill TJ, Yarowsky PJ, Krueger BK (1993) Mutually exclusive exon splicing of type III brain sodium channel alpha subunit RNA generates developmentally regulated isoforms in rat brain. *J Biol Chem* 268: 18648–18653.
- Sarao R, Gupta SK, Auld VJ, Dunn RJ (1991) Developmentally regulated alternative RNA splicing of rat brain sodium channel mRNAs. *Nucleic Acids Res* 19: 5673–5679.
- Choi JS, Cheng X, Foster E, Leffler A, Tyrrell L, et al. (2010) Alternative splicing may contribute to time-dependent manifestation of inherited erythromelalgia. *Brain* 133: 1823–1835.
- Chatelier A, Dahllund L, Eriksson A, Krupp J, Chahine M (2008) Biophysical properties of human $\text{Na}_v1.7$ splice variants and their regulation by protein kinase A. *J Neurophysiol* 99: 2241–2250.
- Raymond CK, Castle J, Garrett-Engle P, Armour CD, Kan Z, et al. (2004) Expression of alternatively spliced sodium channel alpha-subunit genes. Unique splicing patterns are observed in dorsal root ganglia. *J Biol Chem* 279: 46234–46241.
- Patino GA, Isom LL (2010) Electrophysiology and beyond: Multiple roles of Na^+ channel beta subunits in development and disease. *Neurosci Lett*.
- Scheinman RI, Auld VJ, Goldin AL, Davidson N, Dunn RJ, et al. (1989) Developmental regulation of sodium channel expression in the rat forebrain. *J Biol Chem* 264: 10660–10666.
- Gorter JA, van Vliet EA, Aronica E, Breit T, Rauwerda H, et al. (2006) Potential new antiepileptogenic targets indicated by microarray analysis in a rat model for temporal lobe epilepsy. *J Neurosci* 26: 11083–11110.
- Dib-Hajj SD, Yang Y, Waxman SG (2008) Genetics and molecular pathophysiology of $\text{Na}_v1.7$ -related pain syndromes. *Adv Genet* 63: 85–110.
- Momin A, Wood JN (2008) Sensory neuron voltage-gated sodium channels as analgesic drug targets. *Curr Opin Neurobiol* 18: 383–388.
- Cox JJ, Reimann F, Nicholas AK, Thornton G, Roberts E, et al. (2006) An SCN9A channelopathy causes congenital inability to experience pain. *Nature* 444: 894–898.
- Dib-Hajj SD, Black JA, Waxman SG (2009) Voltage-gated sodium channels: therapeutic targets for pain. *Pain Med* 10: 1260–1269.
- Fertleman CR, Baker MD, Parker KA, Moffatt S, Elmslie FV, et al. (2006) SCN9A mutations in paroxysmal extreme pain disorder: allelic variants underlie distinct channel defects and phenotypes. *Neuron* 52: 767–774.
- Yang Y, Wang Y, Li S, Xu Z, Li H, et al. (2004) Mutations in SCN9A, encoding a sodium channel alpha subunit, in patients with primary erythromelalgia. *J Med Genet* 41: 171–174.
- Ellerkmann RK, Remy S, Chen J, Sochivko D, Elger CE, et al. (2003) Molecular and functional changes in voltage-dependent Na^+ channels following pilocarpine-induced status epilepticus in rat dentate granule cells. *Neuroscience* 119: 323–333.
- Cummins TR, Howe JR, Waxman SG (1998) Slow closed-state inactivation: a novel mechanism underlying ramp currents in cells expressing the hNE/PN1 sodium channel. *J Neurosci* 18: 9607–9619.
- Fletcher EV, Kullmann DM, Schorge S (2011) Alternative splicing modulates inactivation of type 1 voltage-gated sodium channels by toggling an amino acid in the first S3–S4 linker. *J Biol Chem* 286: 36700–36708.
- Brackenbury WJ, Isom LL (2011) Na Channel beta Subunits: Overachievers of the Ion Channel Family. *Front Pharmacol* 2: 53.
- Lopez-Santiago LF, Brackenbury WJ, Chen C, Isom LL (2011) Na^+ channel *Scn1b* gene regulates dorsal root ganglion nociceptor excitability in vivo. *J Biol Chem* 286: 22913–22923.

22. Choi JS, Dib-Hajj SD, Waxman SG (2006) Inherited erythralgia: limb pain from an S4 charge-neutral Na channelopathy. *Neurology* 67: 1563–1567.
23. Cummins TR, Dib-Hajj SD, Waxman SG (2004) Electrophysiological properties of mutant Nav1.7 sodium channels in a painful inherited neuropathy. *J Neurosci* 24: 8232–8236.
24. Fischer TZ, Gilmore ES, Estacion M, Eastman E, Taylor S, et al. (2009) A novel Nav1.7 mutation producing carbamazepine-responsive erythromelgia. *Ann Neurol* 65: 733–741.
25. Jarecki BW, Sheets PL, Xiao Y, Jackson JO, 2nd, Cummins TR (2009) Alternative splicing of Na(V)1.7 exon 5 increases the impact of the painful PEPD mutant channel I1461T. *Channels (Austin)* 3: 259–267.
26. Thun J, Persson AK, Fried K (2009) Differential expression of neuronal voltage-gated sodium channel mRNAs during the development of the rat trigeminal ganglion. *Brain Res* 1269: 11–22.
27. Blackburn-Munro G, Fleetwood-Walker SM (1999) The sodium channel auxiliary subunits beta1 and beta2 are differentially expressed in the spinal cord of neuropathic rats. *Neuroscience* 90: 153–164.